

Emission of Prompt Neutrons in the Thermal Neutron Fission of U^{235}

S. S. KAPOOR, R. RAMANNA, AND P. N. RAMA RAO
Atomic Energy Establishment, Trombay, Bombay, India
 (Received 11 February 1963)

The energy distributions of the prompt neutrons emitted along the direction of motion of the light and heavy fragments have been measured in the laboratory system by the time-of-flight method. A gridded ionization chamber is used to measure the kinetic energies of the fission fragments and their directions of motion with the electric field direction of the ion chamber. A photomultiplier associated with the chamber detects the scintillations in the gas by the passage of a fragment and gives the zero-time pulse. A fast neutron detector placed along the electric field direction of the ion chamber determines the time-of-flight of the prompt neutrons in coincidence with the selected fission events. From the energy distributions in the laboratory system, the emission spectra of the prompt neutrons from the selected light and heavy fragments have been obtained. It is found that for the selected region, the light fragments emit about 30% more neutrons than the heavy fragments and also the average emission energy from the light fragments is about 32% more than that from the heavy fragments. The average nuclear temperatures of the fragments determined from the emission spectra are consistent with the average excitation energies expected from the number of neutrons and gamma rays emitted from the fragments. It is established that the emission spectrum from each fragment is a superposition of the various evaporation spectra corresponding to a distribution of nuclear temperatures. A linear distribution of temperatures up to a certain maximum temperature is found to fit the observed emission spectra. The angular correlations of the prompt neutrons of four different average energies and the light fission fragments have also been determined experimentally. The analysis shows that about 10% of the prompt neutrons are not emitted from the moving fragments. These prescission neutrons have an evaporation-like spectrum and an average energy of about 3.2 MeV. It is proposed that these neutrons are evaporated from the excited fissioning nucleus at stages between the saddle point and the scission.

I. INTRODUCTION

IT is well established from previous studies that immediately after scission of the fissioning nucleus, the fission fragments are formed in states of high-excitation energies and also acquire high-kinetic energies owing to the Coulomb repulsion. The various observations on the prompt neutrons and gamma rays emitted during the de-excitation of the fission fragments have been interpreted^{1,2} on the evaporation model of Weisskopf.³ Terrell² has shown that the calculations based on the evaporation model after taking into account the distribution of nuclear temperatures of the fission fragments are in good agreement with the experimentally observed energy distribution of the prompt neutrons in the laboratory system. In the calculations,² the center-of-mass spectrum of the prompt neutrons (emission spectrum) was also derived from the evaporation theory.³ A direct experimental determination of the emission spectra from the fragments is, however, desirable to verify the proposed theories and also to determine experimentally the distribution of nuclear temperatures of the fragments. An accurate knowledge of the neutron spectra from light and heavy fragments separately is also necessary to compute the expected angular correlation of the prompt neutrons and fission fragments on the assumption that these are all evaporated isotropically from the fully accelerated fragments.

Recent experiments⁴⁻⁶ have shown that the number of neutrons emitted from individual fragments varies in a complicated way with the mass number of the emitting fragments. These results indicate that the average excitation energy and, hence, the average nuclear temperature is a function of the mass number of the emitting fragment. The determination of the emission spectra of the neutrons from fragments of specified masses will directly give the average nuclear temperatures of the fragments of various masses. If the evaporation theory is strictly applicable, the experimentally determined average nuclear temperatures of the fragments must correspond to the average excitation energies of the fragments as measured from the number of neutrons and gammas from fragments of different masses.

In the present paper, the emission spectra of the prompt neutrons from light and heavy fragments separately have been determined from the measurements on the laboratory energy distributions of neutrons emitted along the direction of motion of the light and heavy fragments, respectively. It is established that the emission spectrum from each fragment is a superposition of the various evaporation spectra corresponding to a distribution of nuclear temperatures. The measurements also indicate that a linear distribution of temperatures up to a certain maximum cutoff temperature is sufficient to describe each of the spectra. The measurements on the angular correlation of the prompt neutrons of various specified neutron energies and fission frag-

¹ N. Feather, U. S. Atomic Energy Commission Document BR 335A, 1942 (unpublished).

² J. Terrell, Phys. Rev. **113**, 527 (1959).

³ V. F. Weisskopf, Phys. Rev. **52**, 295 (1937); J. M. Blatt and V. F. Weisskopf, *Theoretical Nuclear Physics* (John Wiley & Sons, Inc., New York, 1952), pp. 365-374.

⁴ S. L. Whetstone, Jr., Phys. Rev. **114**, 581 (1959).

⁵ V. F. Apalin, Yu. P. Dobrynin, V. P. Zakharova, I. E. Kutikov, and L. A. Mikaelyan, At. Energ. (U.S.S.R.) **8**, 15 (1960) [translation: Soviet J. At. Energy **8**, 10 (1961)].

⁶ J. Terrell, Phys. Rev. **127**, 880 (1962).

ments are fitted with the computed distributions using the measured emission spectra to determine the percentage, if any, of the prompt neutrons emitted before scission or from fragments before they acquire their full velocities.

II. THEORY OF THE METHOD

It is usually assumed that in the case of thermal fission all the prompt neutrons are emitted from moving fragments after the fragments have acquired their full velocities under Coulomb repulsion. The analysis^{7,8} of the early measurements on angular correlation of prompt neutrons and fission fragments are in agreement with this assumption. Some justification for this assumption is provided by some of the observations described below. If a fraction of the prompt neutrons is not emitted from the fully accelerated moving fragments, there will be lesser correlation between the neutrons and fragments than calculated on the basis of the above assumption. A comparison between the calculated and experimental distributions will give the extent of the justification of the above assumption. If this fraction of the neutrons is small, the transformation of the energy distributions from laboratory system to the emitting fragment system on this assumption still remains approximately valid.

If a neutron is emitted from a moving fragment whose kinetic energy per nucleon is E_f , the emission energy η and emission angle ψ of the neutron are related with the laboratory energy E and the laboratory angle θ , as follows:

$$\eta = E + E_f - 2(EE_f)^{1/2} \cos\theta, \quad (1)$$

$$\psi = \tan^{-1} [r \sin\theta / (r \cos\theta - 1)], \quad (2)$$

where $r = (E/E_f)^{1/2}$ and $E_f = \frac{1}{2}MV_f^2$. V_f is the velocity of the fragment and M is the mass of neutron. The terms emission energy and emission angle refer to the center-of-mass system which can be taken the same as the fragment system. Transformation of the distribution from the center-of-mass system to the laboratory system gives the following:

$$F(E, \theta) = (E/\eta)^{1/2} G(\eta, \psi), \quad (3)$$

where $F(E, \theta)$ and $G(\eta, \psi)$ are the number of neutrons per fission per unit energy interval and solid angle in the laboratory and center-of-mass systems, respectively.

Substituting

$$G(\eta, \psi) = f(\psi)N(\eta),$$

one gets

$$F(E, \theta) = (E/\eta)^{1/2} f(\psi)N(\eta). \quad (4)$$

The observed distribution $P_L(E, \theta)$ of the neutrons in coincidence with the light fragments is given by

$$P_L(E, \theta) = F_L(E, \theta) + F_H(E, \pi - \theta), \quad (5)$$

where

$$F_L(E, \theta) = (E/\eta_L)^{1/2} f(\psi_L)N_L(\eta_L),$$

$$F_H(E, \pi - \theta) = (E/\eta_H)^{1/2} f(\psi_H)N_H(\eta_H),$$

$$\eta_L = E + E_f^L - 2(EE_f^L)^{1/2} \cos\theta,$$

and

$$\eta_H = E + E_f^H + 2(EE_f^H)^{1/2} \cos\theta,$$

the subscripts L and H refer to light and heavy fragments, respectively. Because of the presence of a strong angular correlation between the fragments and the neutrons for small values of θ , say, up to 20° , the contribution of the second term is less than a few percent for lower E values and decreases to much smaller values for higher E values. The second term can, therefore, be neglected to a first approximation, without causing any appreciable error, as shown later.

Further, for small values of θ i.e., $\cos\theta \approx 1$ the variation in ψ_L and thereby in $f(\psi_L)$ for various values of E is expected to be negligible if the anisotropy of emission is not significantly large. With these assumptions one gets

$$P_L(E, \theta) = (E/\eta_L)^{1/2} N_L(\eta_L). \quad (6)$$

Similarly, the observed distribution of the neutrons in coincidence with the heavy fragments is given by

$$P_H(E, \theta) = (E/\eta_H)^{1/2} N_H(\eta_H). \quad (7)$$

This determines the emission spectra from light and heavy fragments from the measured $P(E, \theta)$ distributions by the following relations:

$$N_L(\eta_L) = P_L(E, \theta) (\eta_L/E)^{1/2}, \quad (8)$$

$$N_H(\eta_H) = P_H(E, \theta) (\eta_H/E)^{1/2}. \quad (9)$$

The average number of neutrons per fission from light and heavy fragments are obtained from Eqs. (8) and (9) as follows:

$$\bar{\nu}_L = \int_0^\infty N_L(\eta_L) d\eta_L, \quad (10)$$

and

$$\bar{\nu}_H = \int_0^\infty N_H(\eta_H) d\eta_H. \quad (11)$$

$P(E, \theta)$ is obtained from the observed time-of-flight distribution by

$$P(E, \theta) = \frac{N(t, \theta) dt}{\Delta E_i \epsilon(E) \omega x}, \quad (12)$$

$$E_{MeV} = \left(\frac{72.3D}{t} \right)^2,$$

where t is the time-of-flight of the neutron in nano-seconds. $N(t, \theta)$ is the number of neutrons detected between time t and $t + dt$ at an angle θ with the direction of motion of the specified fragment. ΔE_i is the corresponding energy interval. ω is the solid angle subtended by the neutron counter at the U^{235} foil. x is the corre-

⁷ R. Ramanna, R. Chaudhry, S. S. Kapoor, K. Mikke, S. R. S. Murthy, and P. N. Rama Rao, Nucl. Phys. **25**, 136 (1961).

⁸ J. S. Fraser, Phys. Rev. **88**, 536 (1952).

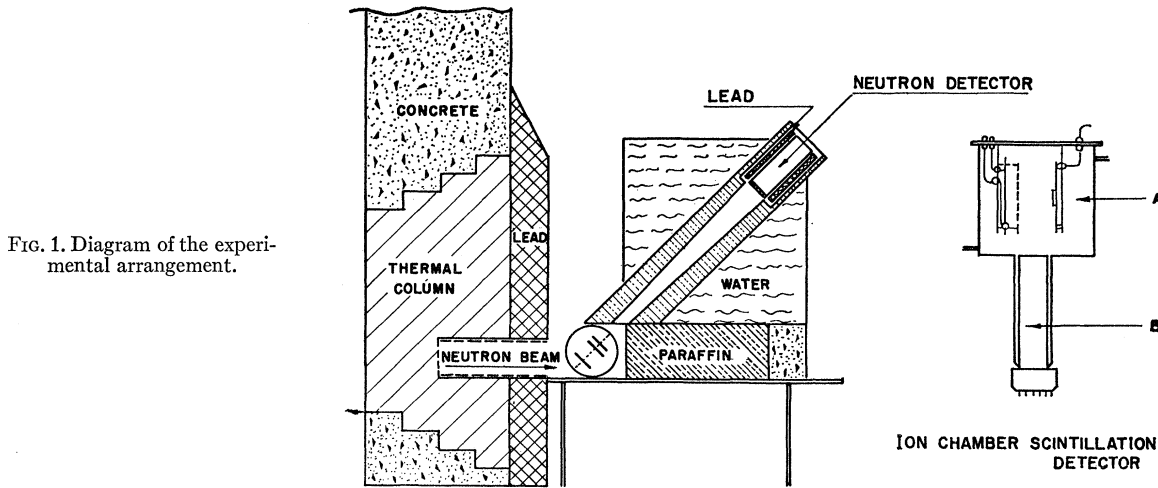


FIG. 1. Diagram of the experimental arrangement.

sponding total number of fission events. $\epsilon(E)$ is the efficiency of the neutron detector for neutrons of energy E . D is the flight path of the neutrons in meters.

The time-of-flight distribution of neutrons for all fragments without reference to their flight directions gives the prompt fission neutron spectrum. The fission neutron spectrum for the case of thermal fission of U^{235} is known² to be best represented by a Maxwellian distribution $N(E) = AE^{1/2}e^{-E/T}$ corresponding to a temperature of $T = 1.29$ MeV. The efficiency $\epsilon(E)$ of the detector can be determined by comparing the observed energy distribution with the Maxwellian distribution with $T = 1.29$ MeV. Efficiency $\epsilon(E)$ is given by

$$\epsilon(E) = \frac{N(t)dt}{\Delta E_i A E^{1/2} e^{-E/T}} \quad (13)$$

with

$$A \int_0^\infty E^{1/2} e^{-E/T} dE = \bar{\nu} x \omega,$$

where $\bar{\nu}$ is the average number of neutrons emitted per fission.

III. EXPERIMENTAL DETAILS

It is necessary to collimate the fission fragments in a fixed direction if the prompt neutrons are to be detected at fixed angles with the direction of motion of the selected fragments. If fission fragment velocities are measured by the time-of-flight technique this is possible by detecting the fragments in a narrow solid angle at the end of a long flight path. If a gridded ionization chamber is used to determine the energy of the fission fragments, a metal system is generally used to collimate the fragments. In both the methods the intensity of the fission fragments is reduced severely. However, using a gridded ionization chamber a method has been developed to determine the kinetic energies and also the angles of the fission fragment tracks, with respect to the

electric field direction of the ionization chamber without the use of a collimator. The prompt neutrons are detected along the electric field direction by means of a plastic scintillator and in coincidence with the fragments of selected energy and angle. The energies of the prompt neutrons are obtained by measuring their time of flights over a fixed distance. In this way, the time-of-flight distributions of the prompt neutrons at selected angles with the direction of the fission fragments of selected energies are obtained.

Figure 1 shows the experimental arrangement. A is a gridded ionization chamber and the fission scintillations are observed by the photomultiplier B. The grid cathode distance (d_{gc}) and the grid collector distance (d_{ga}) are 2.1 and 0.7 cm, respectively. The cathode of the ionization chamber is coated with a layer of U^{235} of thickness $100 \mu\text{g}/\text{cm}^2$. The chamber is filled with pure xenon gas at a pressure of 65 cm of mercury. The photomultiplier, B, covered with a very thin layer of *p*-quaterphenyl is used to observe the scintillations produced in the xenon gas by the passage of fission fragments. The xenon

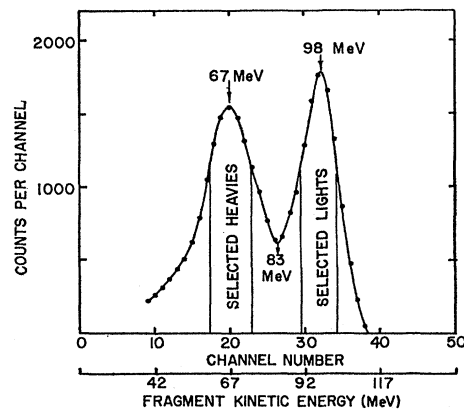


FIG. 2. Kinetic energy distribution of the fission fragments obtained from the gridded ionization chamber.

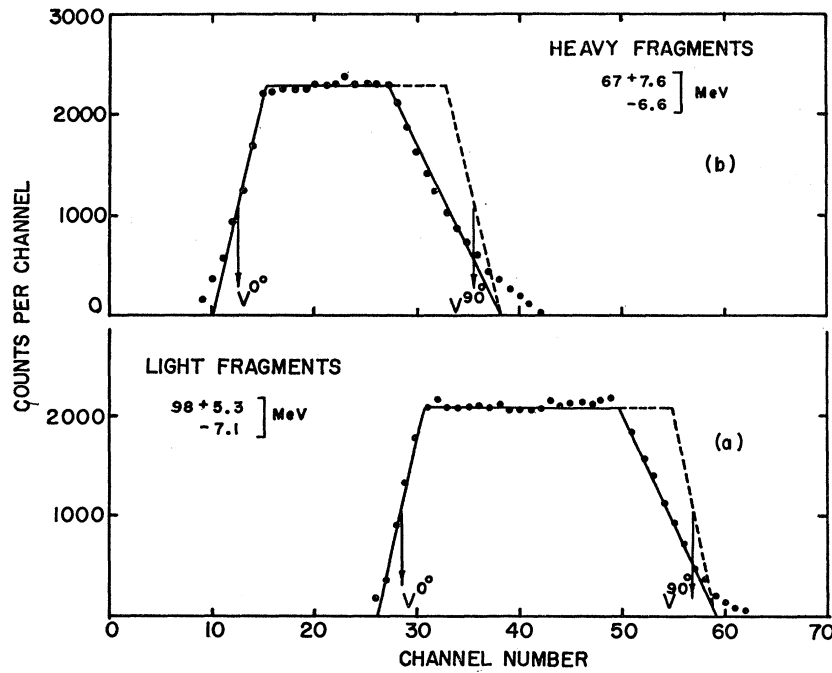


FIG. 3. Pulse-height distribution of the grid pulses for the selected light and heavy fragments.

scintillations give the zero time for the time-of-flight measurement of the prompt neutrons. The xenon gas is purified by passing it over hot calcium to remove any traces of moisture and then solidifying it in a liquid-nitrogen trap while traces of gaseous impurities are removed by pumping. The purifying operation is repeated several times to ensure a high degree of purity. The electric fields between the cathode and the grid, and the grid and the collector, are chosen for the optimum conditions⁹ such that recombination in the cathode grid region and electron capture by the grid structure is negligible. To avoid the dependence¹⁰ of the gain of the linear amplifier on the pulse rise times, a delay line shaped amplifier having a flat top of 10 μ sec was used.

A. Measurement of the Angle of the Fission Tracks

Several workers have used ionization chambers to measure the angles of the tracks of heavily ionizing particles with the electric field direction of the chamber. In a previous method,^{7,11} the angle was obtained by determining the delay between the instant of formation of the track and the instant of pulse rise at the anode, for the tracks of the same range. However, an alternate method has been used here to determine the angular

distribution of the fission fragments based on the fact that the amplitude of the grid pulse varies linearly with $\cos\theta$, where θ is the angle of the track with the field direction. In the present work, it is found that for the case of fission fragments, the loss of energy resolution caused by the simultaneous extraction of pulses from the grid and the collector is not significant because of the larger inherent energy spread present due to the source thickness itself. The addition of a second grid in the chamber was therefore not necessary. The ionization spectra of the fission fragments as obtained from the collector pulses with and without extracting pulses from the grid were found to be the same. Figure 2 shows the ionization spectrum of fission fragments. The energy calibration is done by the known positions of the light and heavy peaks after correcting for ionization defects. The negative pulse height at the grid due to electron collection is given by

$$V_g = (Q_0/C_g)[1 - (R^* \cos\theta/d_{cg})], \quad (14)$$

where Q_0 is the total charge of the electrons, C_g is the capacity of the grid, and R^* is a quantity which depends on the range of the fragment and independent of θ .

For a fixed range, Eq. (14) gives

$$N(V_g)dV_g = \text{const}n(\theta)dV_g. \quad (15)$$

The grid pulse-height distribution for a fixed energy of the fragments, therefore, gives the angular distribution of the fragments with the electric field direction. For isotropic emission of fragments of fixed energy (and, therefore, fixed R^*) the grid pulse-height distribution is rectangular and ranges from $V_g^{\min} = (Q_0/C_g)[1 - (R^*/d_{cg})]$

⁹ O. Bunemann, T. E. Cranshaw, and J. A. Harvey, Can. J. Res. **27**, 191 (1949).

¹⁰ D. H. Wilkinson, *Ion Chambers and Counters* (Cambridge University Press, New York, 1950), p. 103.

¹¹ R. Ramanna, R. Chaudhry, S. S. Kapoor, K. Mikke, S. R. S. Murthy, and P. N. Rama Rao, in *Proceedings of the Conference on Nuclear Electronics, Belgrade, 1961* (I.A.E.A., Vienna, 1962), Vol. 1, p. 303.

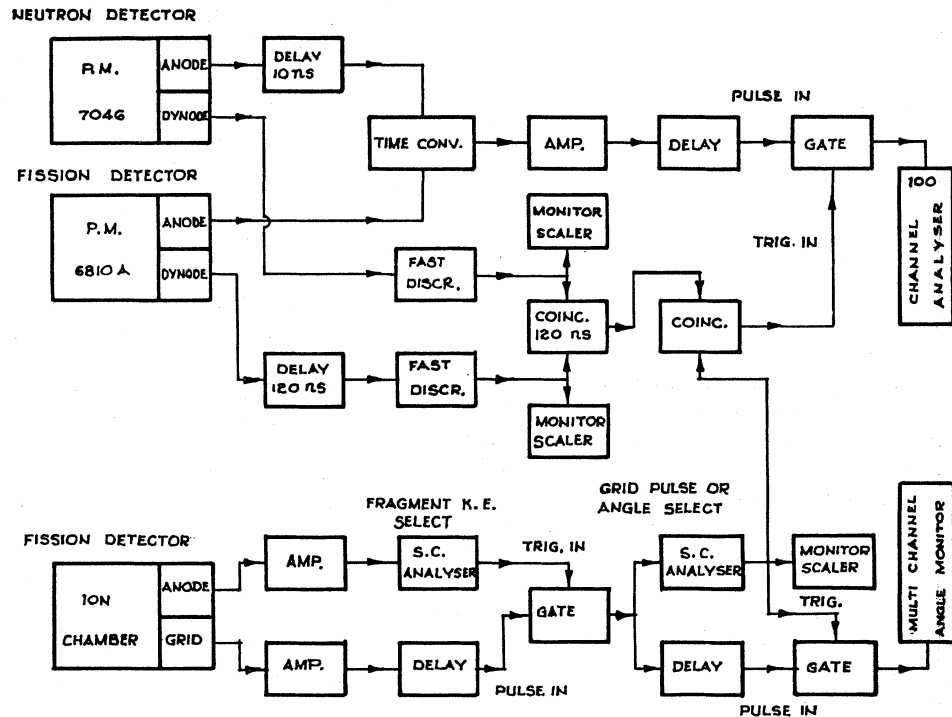


FIG. 4. Block diagram of the electronic arrangement to obtain the time-of-flight spectra of the prompt radiations at selected angles with the direction of motion of the fission fragments of selected energies.

$= V_0^\circ$ to $V_0^{\max} = Q_0/C_0 = V_{90^\circ}$ corresponding to the emissions parallel and perpendicular to the electric field direction of the chamber. The angle of the track with the electric field direction is given by

$$\cos\theta = (V_{90^\circ} - V_0) / (V_{90^\circ} - V_0^\circ), \quad (16)$$

where V_0° and V_{90° can be obtained from the rectangular distribution for the fixed energy of the fragments. The main factors which distort the pulse-height distribution of the grid pulses from the expected shape are (a) bandwidth of the linear amplifier, (b) the finite energy width of the selected fragments and the straggling of the range, and (c) the finite thickness and nonuniformity of the source. An analytical treatment by Ogawa *et al.*¹² shows that the grid pulses can be amplified with a fair degree of linearity together with a good signal-to-noise ratio, if the differentiating and integrating time constants T_1 and T_2 , respectively, of the amplifier are chosen such that $T_1 \gg T \gtrsim T_2$, where T is the maximum rise time of the pulses. The factor (b) modifies the rising edge of the rectangular distribution due to the mixing of the various ranges. The factor (c) causes a reduction in the counts at angles approaching 90° , due to the loss of fragments in the source material. In the present case, the maximum rise time of the grid pulses was about $5 \mu\text{sec}$ and T_1 and T_2 were chosen to be 80 and $5 \mu\text{sec}$, respectively.

The grid pulse-height distribution of light and heavy fission fragments selected at the peaks of the kinetic-

energy distribution corresponding to kinetic energies $98_{-7.1}^{+5.3}$ MeV and $67_{-6.6}^{+7.6}$ MeV are shown in Fig. 3. For a small spread in the selected range of fragments and in the absence of the foil thickness effects, the distribution should have the same rise and fall. The pulse heights corresponding to half the maximum rise and half the expected fall have been chosen as average V_0° and V_{90° for the average range of the selected fragments. The average values of $\cos\theta$ were then calculated for a narrow range of selected pulse heights using Eq. (16). The average values of $\cos\theta$ are not sensitive to the choice of V_{90° whether it is chosen at the half-maximum of the fall in the experimental distribution or of the expected fall for very thin foils.

B. Measurement of the Prompt Neutron Energies

The prompt neutron energies were measured by the time-of-flight method. The fast neutron detector was a plastic scintillator of 10-cm diam and 4-cm thickness and was kept at a distance of 1.03 m along the electric field direction of the chamber. The time difference between the zero-time pulse and the neutron-detector pulse was converted into pulse height by a time-to-pulse-height converter.¹³ The time converter was calibrated by delaying the neutron-detector pulses by calibrated delay lines and noting the position of the prompt gamma peak for each delay, and was found to be linear for the time range from 0 to 120 nsec.

The side channel discriminator outputs of the two

¹² I. Ogawa, T. Doke, and M. Tsukuda, Nucl. Instr. Methods 13, 169 (1961).

¹³ J. B. Garg, Nucl. Instr. Methods 6, 72 (1960).

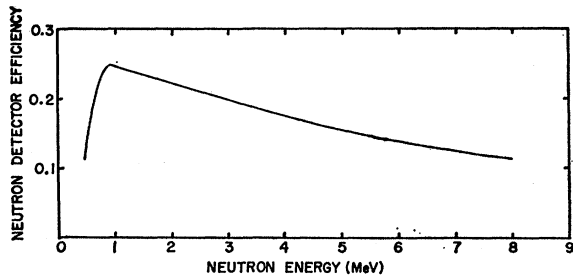


FIG. 5. Measured neutron detection efficiency of the prompt radiation detector.

photomultipliers were fed to a slow coincidence unit of 120-nsec resolution time which was used to gate the output of the time converter. The side channel discriminators were set to cut off the photomultiplier noise in the neutron detector and pulses due to alpha scintillations in the photomultiplier B. Since the time converter was of the overlapping type the accidental coincidences are, therefore, due to the background pulses arriving both before and after the zero-time pulses. The coincidences due to the negative time pulses were avoided by delaying the side channel zero-time pulses by a time equal to the time resolution of the slow coincidence unit. The accidental counts/channel due to chance coincidences are given by $N_1 N_2 \tau$, where N_1 and N_2 are the counting rates of fission scintillations and neutron detector pulses, respectively, and τ is the time width of the channel. As shown in Fig. 1, the neutron detector was well shielded to reduce the background counts N_2 in the neutron detector. An improved ratio of the true-to-accidental coincidences was obtained at the cost of some reduction in the detection efficiency by covering the plastic scintillator with about 2 cm of lead. The background was determined by placing a shadow cone between the foil and the neutron detector. The background spectrum recorded in this way was found to be the same as that obtained due to the chance coincidences for the same input counting rates. This showed that, with the geometry of detection employed, the time-dependent background due to neutrons detected after single or multiple scattering did not have any appreciable contribution and the major contribution was due to the chance coincidences.

Figure 4 shows the block diagram of the electronic arrangement to obtain the time-of-flight spectra of the prompt radiations at selected angles with the direction of motion of fission fragments of selected energies. The grid pulses corresponding to the fragments of selected energy and angle with the flight direction of the neutrons, gate the time-of-flight distribution. The gated spectrum was displayed on a 100-channel pulse-height analyzer. The total number of selected fission events were simultaneously monitored. The position of the prompt gamma peak which corresponds to 3.5 nsec flight time was used to determine the zero time. The width of the gamma peak which was found to be about

5.5 nsec gives the time resolution. The time-of-flight distributions of the neutrons were converted into the energy distributions using Eq. 12. The flight path used in the calculation was $D = D_0 + \bar{d}$, where D_0 is the distance of the face of the detector from the uranium foil and \bar{d} is the average scattering length of the neutrons in the scintillation crystal. In the present calculations the value of D used was $1.03 + 0.02 = 1.05$ m.

The time-of-flight distribution of all the fission events after correcting for accidental coincidences determined the efficiency of the detector [Eq. (13)]. The detector efficiency was monitored before and after each measurement to ensure that the efficiency did not change during the measurement. Figure 5 shows the efficiency of the detector, as obtained experimentally during the time-of-flight measurement in coincidence with the selected light fragments. The prompt neutron time-of-flight distribution along the direction of motion of the heavy fragments was measured with a slightly increased bias of the neutron side channel discriminator, as the noise of the photomultiplier was found to have increased, when these measurements were started. However, the efficiency of the detector was accurately determined and calculations for the heavy fragment data were carried out using this measured efficiency.

For directly determining the angular correlation of the prompt neutrons of selected energies and the selected light fragments, the block diagram of the electronic arrangement was slightly different from that shown in Fig. 4. In this case, the grid pulse-height distribution of the selected light fragments giving the angular distribution of the fragments [Eq. (15)] was gated by the prompt neutrons of the selected energies, and displayed on a multichannel analyzer.

IV. EXPERIMENTAL RESULTS

Figure 6(a) shows the time-of-flight distribution of the prompt neutrons detected at an average angle $\theta = 13^\circ$ with the direction of motion of the light fragments. The contribution of the accidental counts due to background which was found to be constant in time is also shown in the figure. The light fragments were selected at the peak of the kinetic-energy distribution and correspond to energies $98.7_{-1.1}^{+5.3}$ MeV (Fig. 2). The time-of-flight distribution of the prompt neutrons detected at an average angle $\theta = 18^\circ$ with the direction of motion of the heavy fragments selected at the peak with energies $67.6_{-6.6}^{+7.6}$ MeV is shown in Fig. 6(b) after correcting for accidental counts. The corresponding converted energy distributions of the prompt neutrons for the selected light and heavy fragments are shown in Fig. 7. The contribution of the neutrons emitted from the opposite fragments to the experimental points of Fig. 7 was derived using Eq. (5). The emission spectra derived later in the paper were used in the calculations. These contributions to the light fragment spectrum at 1 MeV and heavy fragment spectrum

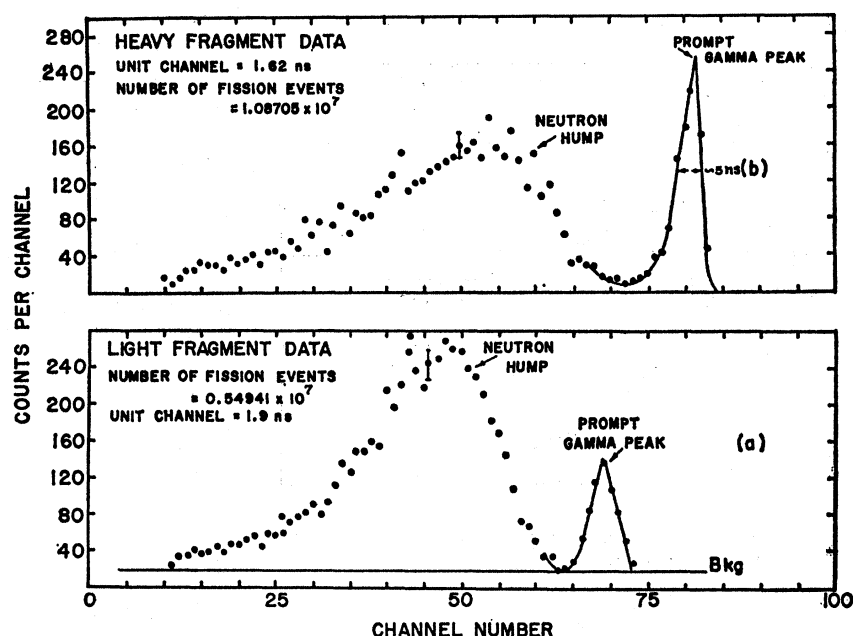


FIG. 6. Time-of-flight distributions of the prompt neutrons in coincidence with (a) the light fragments at $\theta = 13^\circ$ and (b) the heavy fragments at $\theta = 18^\circ$.

at 0.6 MeV were 2 and 3.4%, respectively, decreasing exponentially to almost zero at 3 MeV in each case. These corrections to the experimental points with the available statistics are, therefore, small and do not affect the data. The observed prompt neutron spectrum at $\theta = 13^\circ$ with the light fragment direction is a superposition of two spectra, one due to the neutrons with emission velocities from 0 to ∞ emitted along the direction of motion of the fragments, and the other due to the neutrons with emission velocities from 0 to V_f^L emitted opposite to the fragment direction. The dip in the observed distribution corresponds to the neutrons emitted with zero velocity and appearing in the laboratory with the velocity of the fragment at the time of neutron emission. This dip corresponds to the average selected fragment velocity ($E_f^L = 1.046$ MeV), and may be taken as a justification for the assumption that the fragments attain their full velocities before neutron emission takes place. A similar dip in the spectrum in coincidence with the selected heavy fragments is expected at $E_f^H = 0.486$ MeV, but the measurements were limited to neutron energies up to 0.5 MeV.

The emission spectra for emission from the light and heavy fragments normalized to the same number of fission events were derived from the observed laboratory spectra using Eqs. (8) and (9) with $E_f^L = 1.046$ MeV and $E_f^H = 0.486$ MeV and are shown in Fig. 8. An accurate determination of the masses of the selected fragments require the simultaneous measurement of the kinetic energies of both the fragments. However, from the measurement of the kinetic energies of only single fragments, the masses of the fragments can be roughly determined, assuming a fixed value for the total kinetic energy of the two fragments. If the average total

kinetic energy is taken as $\bar{E}_k = 165$ MeV, it is found that the average masses of the light and heavy fragments are 95_{-9}^{+11} and 139_{-8}^{+10} , respectively. The distribution of the total kinetic energy further increases the range of selection of the masses. From these emission spectra for the selected masses of the light and heavy fragments, the following values are obtained:

$$\begin{aligned} \bar{v}_L &= (1.223 \pm 0.028) & \bar{\eta}_L &= (1.357 \pm 0.050) \text{ MeV} \\ \bar{v}_H &= (0.940 \pm 0.044) & \bar{\eta}_H &= (1.028 \pm 0.065) \text{ MeV} \\ \bar{v} = \bar{v}_L + \bar{v}_H &= (2.163 \pm 0.072) & \bar{\eta} &= (1.3\bar{\eta}_L + \bar{\eta}_H) / 2.3 \\ & & &= (1.214 \pm 0.056) \text{ MeV}. \end{aligned}$$

The value of $\bar{\eta} = (1.214 \pm 0.056)$ MeV obtained from the present measurements is in very good agreement with the value of $\bar{\eta} = 1.18$ MeV derived by Terrell² from the analysis of the measured laboratory energy distributions. The light and the heavy fragments are known⁶ to emit more neutrons in the symmetric and very asymmetric regions, respectively. As the present selection of masses does not include these regions completely, a lower value of $\bar{v} = 2.163 \pm 0.072$ is obtained experimentally. We find that for the selected region of masses, the light fragments emit about 30% more neutrons than the heavy and also the mean emission energy of the neutrons from the light fragments is about 32% more than that from the heavy fragments. The higher value of \bar{v}_L / \bar{v}_H than the ratio expected for all the light and heavy fragments may be due to the selection of masses in which the heavy fragments contain more magic and near-magic nuclei. These results are different from that obtained by Bowman *et al.*,¹⁴ who find that for the case

¹⁴ H. R. Bowman, S. G. Thompson, J. C. D. Milton, and W. J. Swiatecki, *Phys. Rev.* **126**, 2120 (1962).

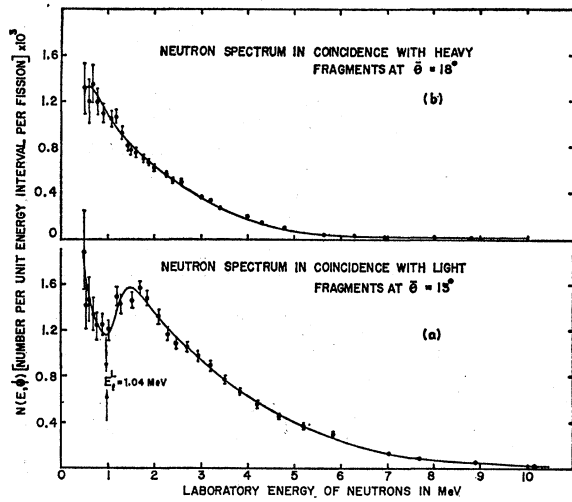


FIG. 7. Energy distributions of the prompt neutrons in coincidence with (a) the light fragments at $\theta = 13^\circ$ and (b) the heavy fragments at $\theta = 18^\circ$.

of spontaneous fission of Cf^{252} , though $\bar{\nu}_L/\bar{\nu}_H = 1.11$, the emission spectra of the neutrons from the light and the heavy fragments are identical.

The angular distributions of the prompt neutrons of the four different mean energies with the direction of motion of selected light fragments are shown in Fig. 9. The experimental points have been corrected for the contribution of the neutrons from the opposite fragments using Eq. (5). The experimentally observed value of $\bar{\nu}_L/\bar{\nu}_H$ and the observed emission spectra from each fragment were used in the calculations. The experimental points, therefore, represent the angular correlation of the light fission fragments and prompt neutrons emitted from the selected light fragments only.

V. DISCUSSION

A. Emission Spectra of Neutrons

On the evaporation model,³ the spectrum of neutrons evaporated from an excited nucleus is

$$N(\eta) = (\eta/T^2)e^{-\eta/T}.$$

The temperature T is obtained from

$$T = (\bar{E}_r/a)^{1/2},$$

where a is the nuclear temperature parameter and \bar{E}_r is the average residual excitation energy given by

$$\bar{E}_r = E_i - E_b - \bar{\eta}.$$

E_i , E_b , and $\bar{\eta}$ are the initial excitation energy, binding energy of a neutron, and the average emission energy of the neutrons, respectively. For emission corresponding to a single temperature T , a plot of $\log[N(\eta)/\eta]$ against η should be linear. Figure 10 shows a plot of $\log_{10}[N(\eta)/\eta]$ against η from the experimental data for the light and heavy fragments, the light fragment data

being reduced by 30%. The experimental points do not lie on a straight line, and show that the emission spectrum from each fragment is a superposition of the various evaporation spectra corresponding to a distribution of nuclear temperatures. A plot of $\log[N(\eta)/\eta^{1/2}]$ against η is shown in Fig. 11 both for the light and heavy fragments. The close similarity of the emission spectrum from each fragment with a Maxwellian distribution as evident from the plot is the reason of the success of a Maxwellian emission spectrum to explain the observed energy distributions of the prompt neutrons in the laboratory system. However, slight deviations show that the emission spectrum is somewhat broader than a single Maxwellian. It was found that each of the emission spectra can be fitted quite accurately with the sum of two normalized Maxwellians differing in their average energies by any value from about 0.5 to 0.8 MeV. In Fig. 11 the experimental points are fitted to the sum of two normalized Maxwellians differing in their average energy by 0.6 MeV. Similar results were obtained in the theoretical analysis of Terrell.² However, there is no fundamental reason to represent the emission spectrum with the sum of two Maxwellians, except that it suitably represents a broad spectrum which is expected from a nucleus with a distribution of nuclear temperatures.

The distribution in the residual excitation energies and thereby in the nuclear temperatures arises from the initial distribution in the excitation energies of the frag-

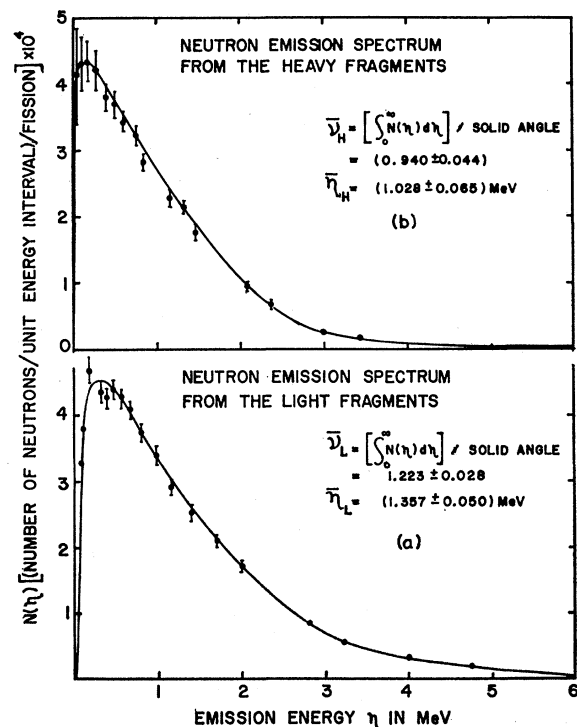


FIG. 8. The emission spectra for emission from (a) the light and (b) the heavy fragments.

ments and due to the various states of excitation in which the fragments are left after the emission of first, second, third, etc., neutrons. The emission spectrum on the evaporation theory for a distribution $P(T)$ of the nuclear temperatures can be written as

$$N(\eta) = \frac{\int \frac{\eta}{T^2} e^{-\eta/T} P(T) dT}{\int P(T) dT} \quad (17)$$

It is, therefore, possible to obtain information on the distribution of nuclear temperatures for emission from the light and heavy fragments, from the measured emission spectra. Evidently the temperature distribution should be limited to a maximum temperature T_m , corresponding to the residual excitation energy after the emission of the first neutron from a state of maximum initial excitation energy of the fragments. Assum-

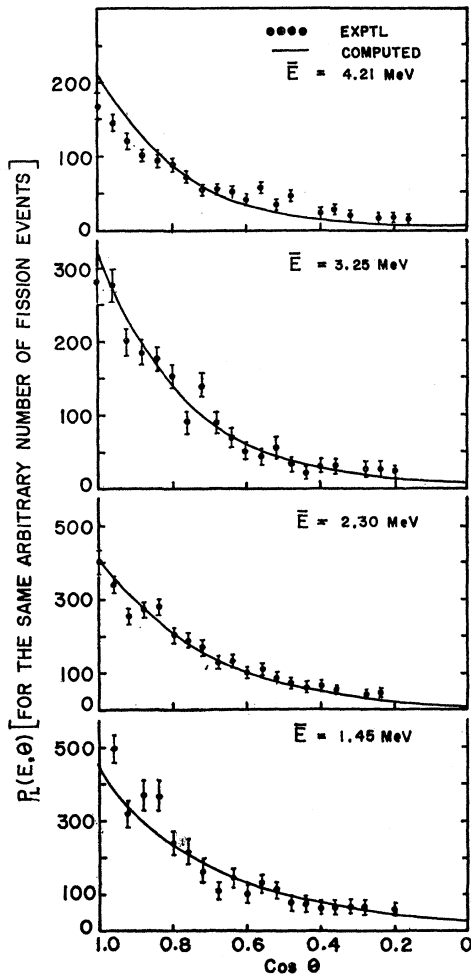


FIG. 9. Angular correlations of the prompt neutrons of the four different mean energies and the selected light fission fragments, for neutrons emitted only from the light fragments.

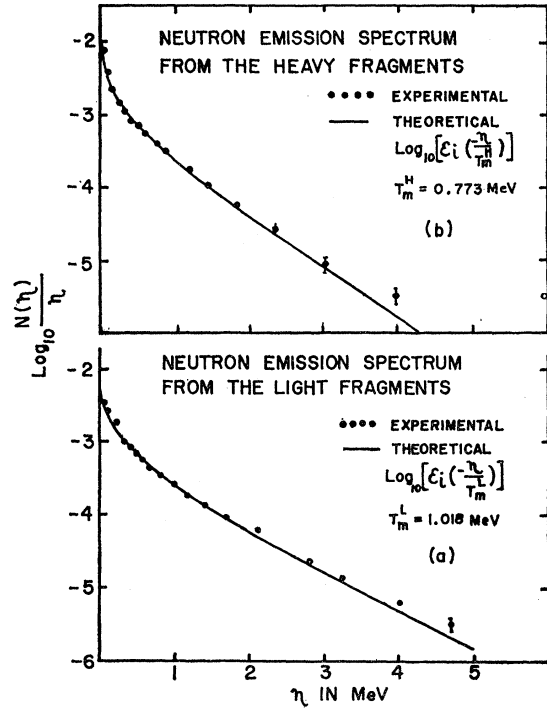


FIG. 10. A plot of $\log_{10}[N(\eta)/\eta]$ against η , for neutrons emitted from (a) the light fragments, and (b) the heavy fragments. The number of neutrons from the light fragments is reduced by 30% to make the total number from the light and heavy fragments equal.

ing that the temperature distribution is linear up to a certain maximum temperature T_m , the expected emission spectrum is given by

$$N(\eta) = \frac{\int_0^{T_m} \frac{\eta}{T^2} e^{-\eta/T} T dT}{\int_0^{T_m} T dT} = -\frac{2\eta}{T_m^2} \text{Ei}\left(-\frac{\eta}{T_m}\right), \quad (18)$$

where

$$\text{Ei}(-z) = \int_{-\infty}^{-z} \frac{e^y}{y} dy; \quad T_m = \frac{3}{4}\bar{\eta}.$$

The theoretical emission spectra calculated from Eq. (18) on the assumption of linear temperature dependence for the case of light and heavy fragments are shown in Fig. 10 along with the experimental points. The maximum temperatures T_m^L and T_m^H correspond to the average emission energies from the light and heavy fragments, respectively, and are $T_m^L = 1.018$ MeV and $T_m^H = 0.773$ MeV. The agreement between the experimental and theoretical distributions is striking. The slight deviation at high energies may be due to the over simplification of the assumed temperature distribution. Terrell² has shown that the initial excitation energies of the single fragments have a Gaussian distribution with an average value equal to the total energy emitted in the form of neutrons and gamma rays,

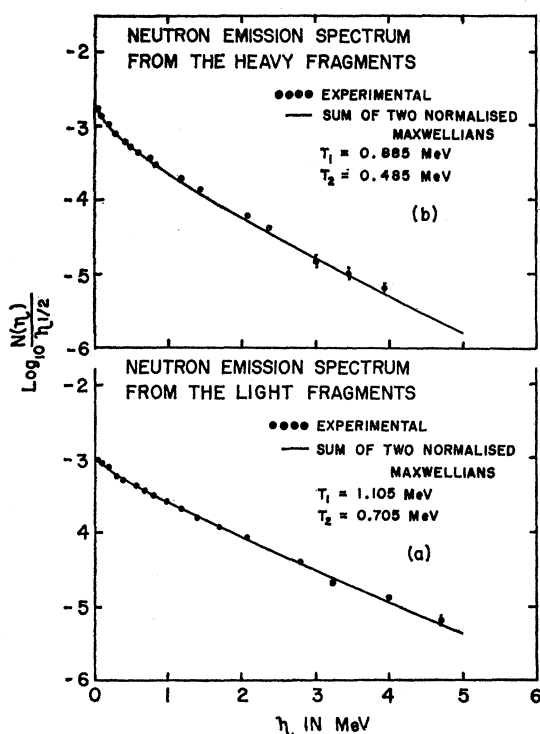


FIG. 11. A plot of $\log_{10}[N(\eta)/\eta^{1/2}]$ against η , neutrons emitted from (a) the light fragments and (b) the heavy fragments.

and an rms deviation which fits the distribution of the number of emitted neutrons. After adding the shifted distributions due to the emission of the first, second, etc., neutrons, the residual energy distribution of the fragments has been obtained. His analysis also shows that the distribution of the nuclear temperatures obtained in this way is similar to a distribution of the linear form $P(T) = 2T/T_m^2$, up to a maximum temperature T_m . For the Gaussian distribution of the initial excitation energy, the rms deviation is such that the maximum residual excitation energy roughly corresponds to the initial average excitation energy. The maximum temperature T_m is, therefore, obtained from

$$aT_m^2 = \bar{E}_i = \bar{\nu}_f(\bar{E}_b + \bar{\eta}) + \bar{E}_\gamma, \quad (19)$$

where $\bar{\nu}_f$ is the average number of neutrons, and \bar{E}_γ is the average energy emitted in the form of gamma rays from the fragment. If one assumes that the nuclear temperature parameter a is proportional to the mass of the emitting nucleus, the expected ratio T_m^L/T_m^H of the maximum temperatures for the light and heavy fragments can be obtained from Eq. (19). Taking the average binding energy of the emitted neutrons to the fragments $\bar{E}_b = 5.4$ MeV, both for the light and heavy fragments (based on Cameron's mass table taking shell effects into account¹⁵), and assuming that equal energy

is emitted in the form of gamma rays from the light and heavy fragments and each equal to 3.6 MeV, we find that $\bar{E}_i^L = 11.86$ MeV and $\bar{E}_i^H = 9.64$ MeV. This gives $T_m^L/T_m^H = 1.34$. The expected ratio of the maximum temperatures, and therefore of the average temperatures of the light and heavy fragments is 1.34. The ratio of the average temperatures of the light and heavy fragments obtained from the observed emission spectra is 1.32. The agreement with the expected ratio is surprisingly good in view of the various assumptions made in the calculations of T_m^L/T_m^H . For instance, it is quite likely that the number of gammas emitted from the light and heavy fragments may not exactly be the same, although there is no reason for the numbers to be very different. Further, on the simple liquid-drop model the binding energies \bar{E}_b^L and \bar{E}_b^H of the neutrons to the light and heavy fragments are 5.7 and 4.7 MeV, respectively. This would give that the average temperature of the light fragments should be higher than that of the heavy fragments by about 40%. In any case, the average temperature of the light fragments is expected to be higher than that of the heavy fragments by a detectable percentage.

The variation of the average emission energies with the mass of the emitting fragment should be expected in view of the neutron emission data from individual fragments,⁶ which show that the average excitation energy of a fragment depends on its mass number. The average neutron emission energies for emission from the individual fragments have been calculated from the corresponding data on the number of neutrons emitted from fragments of different masses, using Eq. (19). The average value of a for the fragments of average mass in the thermal fission of U^{235} was calculated from the equation

$$aT_m^2 = \frac{\bar{\nu}(\bar{E}_b + \bar{\eta}) + \bar{E}_\gamma}{2}.$$

Substituting $\bar{E}_\gamma = 7.2$ MeV, $\bar{\eta} = 1.18$ MeV, $\bar{E}_b = 5.4$ MeV, $\bar{\nu} = 2.43$, and $T_m = \frac{3}{2}\bar{T} = \frac{3}{2}\bar{\eta} = 0.885$ MeV one obtains a value for $a = 14.8$ MeV. Terrell² obtained a value of $a = 12 \pm 2$ MeV by fitting the calculated value of the average energy of the laboratory neutron spectrum with that experimentally observed for the thermal fission of U^{235} . The nuclear temperature parameter a for the emitting fragment was taken as $a = 14.8M_f/M$ where M is the average of the fragment mass distribution and M_f is the mass of the emitting fragment. The calculated variation of the average emission energy with the emitting fragment mass using the neutron emission data of Terrell,⁶ for thermal fission of U^{235} , is shown in Fig. 12. The calculations were done in an iterative way, where initially $\bar{\eta}$ was assumed to be the same for all masses. As there does not exist any experimental data on the energy emitted in the form of gamma rays from each fragment, it was assumed that equal energy is emitted in the form of gamma rays from each fragment. How-

¹⁵ A. G. W. Cameron, Can. J. Phys. 35, 1021 (1957).

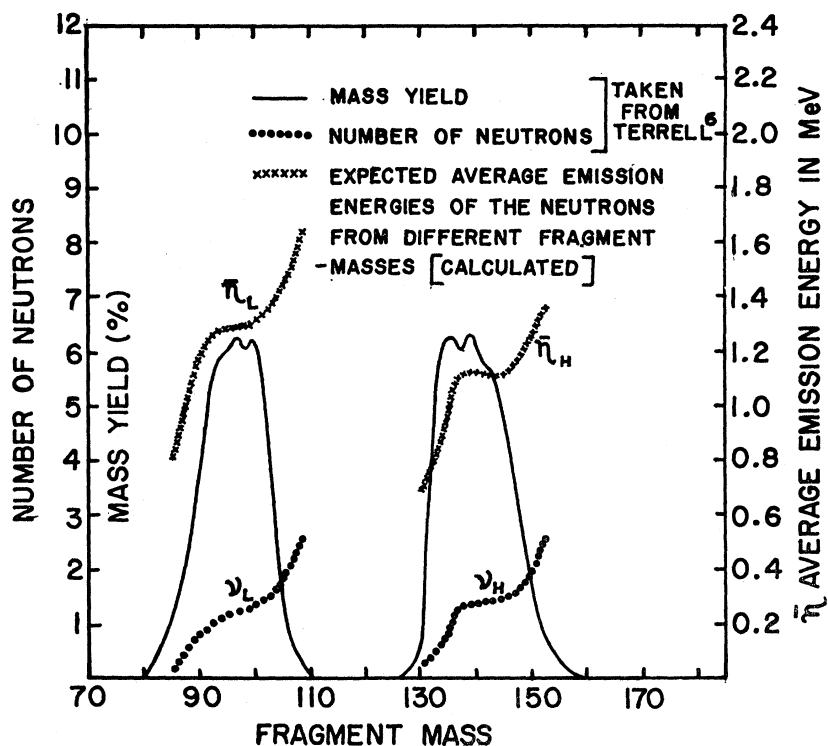


FIG. 12. The expected variation of the average emission energy with the emitting fragment mass calculated from the neutron emission data of Terrell (reference 6).

ever, even if there are small differences in the gamma-ray energies from different fragments, the calculated curve will remain essentially unaltered, unless the differences are very large. An experimental determination of the average emission energies from fragments of specified masses is necessary to verify the assumptions involved in the calculations. Our results for a gross mass selection of the light and heavy fragments definitely predict the existence of the calculated variation, and show that the energies emitted in the form of gamma rays from fragments of various masses are not very different.

However, the recent results of Bowman *et al.*¹⁴ for the case of spontaneous fission of Cf^{252} show that though the light fragments emit about 11% more neutrons than the heavy, the emission spectra for both the light and heavy fragments are identical. The equality of the average temperatures for the light and heavy fragments cannot be reconciled with Eq. (19), until out of the total 9-MeV gamma-ray energy, about 7.0 MeV is emitted by the heavy fragments and only 2.0 MeV by the light fragments. At present, there is no reason to believe such a favored emission of gamma rays from the heavy fragments, when actually the light fragments have a higher internal excitation energy. However, if a considerable number of gamma rays are emitted before the emission of neutrons, the average nuclear temperature as measured by the neutron emission may not reflect the average initial excitation of the fragments. In order to explain the results of Bowman *et al.*¹⁴ on this possi-

bility, one has to assume further that there exists much larger competition between the gamma and the neutron emission in the light fragments than in the heavy fragments. But, at present, there does not exist any theoretical justification for assuming these possibilities.

B. Angular Correlation of Prompt Neutrons and Fission Fragments

A study of the fragment neutron correlations is of importance to determine at what stage of the fission process the emission of the neutrons takes place and the angular distribution of the neutrons in the emitting fragment system. However, to extract this information from the measured angular correlations an exact knowledge of the emission spectra and the neutron emission probabilities from each of the two fragments is required [Eq. (5)]. The previous measurements by Ramanna *et al.*⁷ on angular correlation of prompt neutrons and fission fragments were analyzed assuming a single Maxwellian emission spectrum having an average energy of 1.47 MeV. A value of $\bar{\nu}_L/\bar{\nu}_H=1.3$ was found to give a better fit to the angular distribution data. Terrell⁶ has recently pointed out that if a double Maxwellian emission spectrum with $\bar{\eta}=1.21$ MeV is assumed both for emission from the light and heavy fragments, $\bar{\nu}_L/\bar{\nu}_H=1.0$ gives excellent agreement with these results. The selected region of light fragments in the previous measurements by Ramanna *et al.*⁷ was nearly the same as in new measurements reported here.

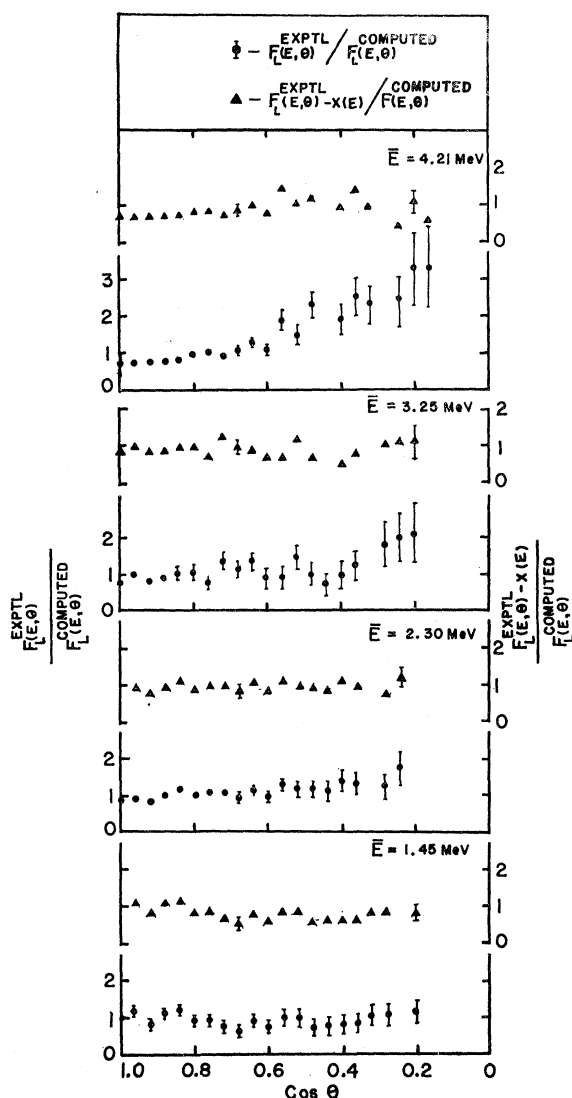


FIG. 13. A plot of $F_L^{\text{exp}}(E, \theta)/F_L^{\text{computed}}(E, \theta)$ against $\cos\theta$, showing the deviations of the experimental angular correlations from the computed ones. A plot of $[F_L^{\text{exp}}(E, \theta) - X(E)]/F_L^{\text{computed}}(E, \theta)$ against $\cos\theta$ also shown in the figure shows that the deviations can be removed after making allowance for the number $X(E)$ of the neutrons emitted prior to scission.

Therefore, analyzing these results with the measured value of $\bar{\nu}_L/\bar{\nu}_H=1.3$ and the observed emission spectra with $\bar{\eta}_L=1.357$ MeV and $\bar{\eta}_H=1.028$ MeV, one finds that the experimentally observed correlations are lesser than expected if all the neutrons are emitted from fully accelerated fragments. Similar results have been obtained by Bowman *et al.*¹⁴ for the case of spontaneous fission of Cf^{252} , who explain these results by assuming that a small fraction of the neutrons is not emitted from the fully accelerated fragments.

The new measurements of the angular distribution of the prompt neutrons of four different mean energies with the direction of motion of the selected light fission

fragments have been analyzed using the measured value of $\bar{\nu}_L/\bar{\nu}_H=1.3$ and $N(\eta) = -(2\eta/T_m^2) \text{Ei}(-\eta/T_m)$ with T_m^L and T_m^H obtained from the experimentally measured emission spectra. The angular correlations of the neutrons emitted only from the light fragments have been obtained by correcting the observed distributions for the fraction $F_H(E, \pi-\theta)/[F_L(E, \theta) + F_H(E, \pi-\theta)]$ emitted by the complementary heavy fragments. The resulting angular distributions of the neutrons of four different mean energies emitted from the light fragments and normalized to the same number of fission events are fitted with the computed $F_L(E, \theta)$ distributions on the assumption of isotropic evaporation [$f(\psi_L)=1$] as shown in Fig. 9. In general, the experimental results are consistent with the assumption of isotropic evaporation from the moving fragments. But in all the cases the experimental distributions show somewhat lesser correlations than the computed $F_L(E, \theta)$ distribution, the disagreement being quite marked for the case of $\bar{E}=4.21$ MeV. A plot of $F_L^{\text{exp}}(E, \theta)/F_L^{\text{computed}}(E, \theta)$ shown in Fig. 13 shows the extent of departure from the computed distributions for the four different energies. In order to remove this discrepancy, one has to assume that a small fraction of the neutrons is not emitted from the moving fragments. Assuming that these neutrons are isotropic in the laboratory system the fraction of such neutrons for different energies have been obtained by deducting from the experimental distributions, $F_L^{\text{exp}}(E, \theta)$, a constant value $X(E)$ which makes $[F_L^{\text{exp}}(E, \theta) - X(E)]/F_L^{\text{computed}}(E, \theta)$ isotropic. As the statistical accuracy of the experimental angular correlations in the 90° region is poor only a rough estimate of the number of these neutrons could be obtained. The isotropic distribution of $[F_L^{\text{exp}}(E, \theta) - X(E)]/F_L^{\text{computed}}(E, \theta)$ obtained in this way for each of the mean neutron energies is also shown in Fig. 13 together with the $F_L^{\text{exp}}(E, \theta)/F_L^{\text{computed}}(E, \theta)$ distribution. The number $X(E)$ of these isotropically emitted neutrons estimated in this way is shown in Fig. 14 as a plot of $\log_{10} X(E)/E$ against E . This analysis shows that these neutrons constitute a fraction of about 10% and are emitted with an evaporation-like spectrum having an average temperature of about 1.6 MeV and, therefore, average energy of about 3.2 MeV. In order to explain accurately the angular distribution data for the case of spontaneous fission of Cf^{252} , Bowman *et al.*¹⁴ also had to assume that about 10% of the neutrons are emitted isotropically in the laboratory system with an average energy of 2.6 MeV.

It has been visualized^{16,17} in the past that a small fraction of the neutrons may be emitted during or just after scission due to the disturbances associated with the breaking of the neck and the retraction of the stumps in a short time into the fragments. Fuller¹⁸ has investi-

¹⁶ D. L. Hill and J. A. Wheeler, Phys. Rev. **89**, 1102 (1953).

¹⁷ V. S. Stavinskii, Zh. Eksperim. i Teor. Fiz. **36**, 629 (1959) [translation: Soviet Phys.—JETP **9**, 437 (1959)].

¹⁸ R. W. Fuller, Phys. Rev. **126**, 685 (1962).

gated in detail the emission of the neutrons related to such processes. However, there exists another possibility of the emission of the neutrons much before scission takes place. The decrease in the potential energy of the fissioning nucleus, after it has crossed the saddle point, is transferred to the various degrees of freedom such as the kinetic energy of motion, excitation energy of the nucleons and the collective deformation of the nuclear surface. The fissioning nucleus is, therefore, in states of high-excitation energy and may also be considered in statistical equilibrium at stages between the saddle point and the scission. It has been shown by Ramanna *et al.*¹⁹ that the emission of the long-range alpha particles can be considered as an evaporation process from the excited fissioning nucleus between the saddle point and the scission. It is, therefore, expected that a small fraction of the prompt neutrons is also emitted between the saddle point and the scission with an evaporation-like spectrum. On the assumption that both the precission neutrons and the long-range alpha particles are evaporated from the compound nucleus, it is possible to compare their relative emission probabilities on the evaporation theory, with that observed experimentally. The average emission width for a particle of mass M is given by

$$\bar{\Gamma} = \frac{1}{\pi^2 \rho_c(\epsilon')} \int_0^\infty \frac{M}{\hbar^2} \epsilon \sigma_c(\epsilon) \omega(\epsilon' - \epsilon) d\epsilon,$$

where

$\rho_c(\epsilon')$ is the level density of the compound nucleus at the excitation energy ϵ' ,

$\sigma_c(\epsilon)$ is the inverse capture cross section,

$\omega(\epsilon' - \epsilon)$ is the density of levels of the residual nucleus at excitation energy $(\epsilon' - \epsilon)$.

On the Fermi gas model

$$\omega(\epsilon' - \epsilon) = \text{const} \exp[2a^{1/2}(\epsilon' - \epsilon)^{1/2}].$$

As the excitation energy of the fissioning nucleus is changing from saddle point to scission point, the probability of finding the nucleus with an excitation energy ϵ' is given by a factor $e^{-\epsilon'/T_D}$, where T_D is some mean distribution temperature as discussed by Ramanna *et al.*¹⁹ Hence,

$$\begin{aligned} \frac{\bar{\Gamma}_\alpha}{\bar{\Gamma}_n} &= \frac{M_\alpha \int_0^\infty \int_\epsilon^\infty \epsilon \sigma_c^\alpha(\epsilon) e^{-\epsilon'/T_D} \exp[2a^{1/2}(\epsilon' - \epsilon)^{1/2}] d\epsilon' \cdot d\epsilon}{M_n \int_0^\infty \int_\epsilon^\infty \epsilon \sigma_c^n(\epsilon) e^{-\epsilon'/T_D} \exp[2a^{1/2}(\epsilon' - \epsilon)^{1/2}] d\epsilon' \cdot d\epsilon} \\ &= \frac{M_\alpha \int_0^\infty \epsilon \sigma_c^\alpha(\epsilon) e^{-\epsilon/T_D} d\epsilon}{M_n \int_0^\infty \epsilon \sigma_c^n(\epsilon) T_D^2 d\epsilon}, \end{aligned} \quad (20)$$

¹⁹ R. Ramanna, K. G. Nair, and S. S. Kapoor, *Phys. Rev.* **129**, 1351 (1963).

where subscripts α , and n refer to alpha particles and neutrons, respectively. Using the values of $\sigma_c(\epsilon)$ as obtained in the previous paper¹⁹ it is found that the observed emission rates are consistent with a value of T of the order of 1 MeV. On the same basis the life time of neutron emission comes out to be 10^{-20} sec which is consistent with the observed number of precission neutrons emitted per fission, if the time from saddle point to scission is also of the same order.

With the available statistics of the measured angular correlations it is not possible to draw any conclusion about the angular distribution of the neutrons in the fragment system, except that the anisotropy of emission, if any, is not large. On the other hand, a small anisotropy of emission of the neutrons of the order of a few percent is expected^{20,7} if the fragments have large angular momenta correlated with their directions of motion, as suggested by Strutinskiĭ.²¹ Investigations on fragment-gamma correlation, to be published elsewhere, show the presence of anisotropy of emission of the prompt gammas in the emitting fragment system. This observation supports the presence of large angular momenta of the fragments and also seeks to resolve the difference in the expected energy in the form of gamma rays on the simple evaporation theory^{22,2} and that obtained from the recent measurements.²³⁻²⁵ Experiments

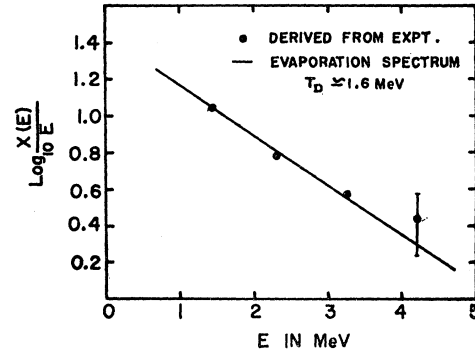


FIG. 14. A plot of $\log_{10} X(E)/E$ against E . $X(E)$ is the number per unit energy interval of the estimated precission neutrons. The last point shows the order of the statistical error involved in the estimation.

²⁰ T. Erikson and V. M. Strutinskiĭ, *Nucl. Phys.* **8**, 284 (1958); **9**, 689 (1958-59).

²¹ V. M. Strutinskiĭ, *Zh. Eksperim. i Teor. Fiz.* **37**, 861 (1959) [translation: *Soviet Phys.—JETP* **10**, 613 (1959)].

²² R. B. Leachman and C. S. Kazek, Jr., *Phys. Rev.* **105**, 1511 (1957).

²³ F. C. Maienschein, R. W. Peele, W. Zobel, and T. A. Love, in *Proceedings of the International Conference on the Peaceful Uses of Atomic Energy* (United Nations, New York, 1958), Vol. 15, p. 366.

²⁴ A. B. Smith, P. R. Fields, A. M. Friedman, S. Cox, and R. K. Sjoblom, in *Proceedings of the International Conference on the Peaceful Uses of Atomic Energy* (United Nations, New York, 1958), Vol. 15, p. 392.

²⁵ H. R. Bowman and S. G. Thompson, in *Proceedings of the International Conference on the Peaceful Uses of Atomic Energy* (United Nations, New York, 1958), Vol. 15, p. 212.

an fragment-gamma correlations are in progress for gamma rays of various average energies to investigate further details of the process.

ACKNOWLEDGMENTS

We are grateful to Dr. J. Terrell for his many valuable comments on this work. We also wish to thank S. R. S. Murthy and B. R. Ballal for their extremely valuable help in many phases of the work, including the

carrying out of the experiment and the maintenance of the electronic equipment. Our thanks are due to D. M. Nadkarni for his help in performing some calculations and for helpful discussions, and to S. L. Raote for the construction of various electronic equipment. We also express our thanks to the Electronics Division for providing us with the pulse-height analyzer and the Radiochemistry Division for the preparation of the uranium foils.

Study of the Radiations Emitted in the Decay of Ni⁶⁵*

J. E. CLINE AND R. L. HEATH

National Reactor Testing Station, Phillips Petroleum Company, Idaho Falls, Idaho

(Received 4 September 1962; revised manuscript received 25 March 1963)

Radiations emitted in the decay of Ni⁶⁵ have been studied using scintillation spectrometry and absolute beta counting. The half-life of this nuclide has been measured to be 2.553 ± 0.008 h. A decay scheme is presented which contains some weak transitions observed to depopulate the higher energy states. Intensities are presented for these transitions and upper limits are placed on intensities of previously reported transitions which were not observed in this work.

I. INTRODUCTION

PROPERTIES of the decay of 2.55-h Ni⁶⁵ have been studied by several experimenters. Swarthout *et al.*¹ and Conn *et al.*² performed early studies of the β -radiation emitted by this nuclide. Siegbahn and Grosh³ reported energies and coincidence relationships for the prominent transitions. More recently, Jambunathan *et al.*⁴ have reported six additional transitions which followed beta branching to higher energy levels. The existence of these levels had previously been established in (p, p') scattering experiments,⁵ but they had not been observed to be excited in the beta decay of Ni⁶⁵.

Three measurements of the directional correlation of the 0.37–1.114-MeV cascade appear in the literature.^{4,6,7} As a result of these measurements, three distinct spin sequences were proposed for the levels in Cu⁶⁵ at 1480 and 1114 keV. Recent Coulomb excitation measure-

ments⁸ have indicated that the spins and parities of the first three known excited levels of Cu⁶⁵ are $\frac{1}{2}^-$, $\frac{5}{2}^-$, and $\frac{7}{2}^-$, respectively. In view of recent interest in core-excitation models of nuclear structure,^{9–12} it is felt that a more complete knowledge of the decay scheme of Ni⁶⁵ and particularly of the intensities of the weaker gamma-ray transitions observed in this decay would aid in the application of these models to this nuclide.

II. EXPERIMENTAL TECHNIQUES AND DATA

1. Source Preparation

Samples of Ni⁶⁵ were produced by irradiation of Ni₂O₃ in a thermal flux facility of the Materials Testing Reactor ($\approx 1.5 \times 10^{13}n/cm^2$ sec). Following irradiation, material was purified using standard Ni chemistry. Sources 3 mm in diameter were prepared for the gamma-ray studies by evaporating Ni in HCl solution, onto 10-mg/cm² plastic films. Liquid sources for the directional-correlation measurement were contained in thin-walled Lucite holders, $\frac{1}{16}$ in. in diameter. Special sources for $4\pi\beta$ counting were prepared from solutions of irradiated Ni, enriched to 99.92% in the Ni⁶⁵ isotope, by deposition on 5 $\mu g/cm^2$ films of VYNS.

* Work performed under the auspices of the U. S. Atomic Energy Commission.

¹ J. A. Swarthout, G. E. Boyd, A. E. Cameron, C. P. Keim, and C. E. Larson, *Phys. Rev.* **70**, 232 (1946).

² E. E. Conn, A. E. Brossi, J. A. Swarthout, A. E. Cameron, R. L. Carter, and D. G. Hill, *Phys. Rev.* **70**, 768 (1946).

³ K. Siegbahn and A. Grosh, *Arkiv Mat. Fys.* **36A**, Nr. 19 (1949).

⁴ R. Jambunathan, M. R. Gunye, and B. Saraf, *Phys. Rev.* **120**, 1839 (1960).

⁵ M. Mazari, W. W. Buechner, and R. P. de Figueiredo, *Phys. Rev.* **108**, 373 (1957).

⁶ T. Wielding and A. Carlson, *Phys. Rev.* **83**, 181 (1951).

⁷ B. Hartmann and I. Asplund, *Arkiv Fysik* **13**, 339 (1958).

⁸ H. E. Gove and B. Elbek, *Bull. Am. Phys. Soc.* **8**, 86 (1962).

⁹ R. D. Lawson and J. L. Uretsky, *Phys. Rev.* **108**, 1300 (1957).

¹⁰ A. deShalit, *Phys. Rev.* **122**, 1530 (1961).

¹¹ B. F. Bayman and L. Silverberg, *Nucl. Phys.* **16**, 625 (1960).

¹² M. Bouten and P. Van Leuven, *Nucl. Phys.* **32**, 499 (1962).